Supporting Information

Effect of Anisotropic Conductivity of Ag_2S-Modified $Zn_mIn_2S_{3+m}$ (m=1, 5) on the Photocatalytic Properties in Solar Hydrogen Evolution

Jingyuan Liu,[*a] Xinyi Xue,[a] Xin Zhou,[a] Gang Chen[a] and Wei Liu[*b]*

a. MIIT Key Laboratory of Critical Materials Technology for New Energy Conversion and Storage, School of Chemistry and Chemical Engineering, Harbin Institute of Technology, Harbin, 150001, China

b. Department of Optical Engineering, Zhejiang A&F University, Hangzhou, 311300, China

THE CONTENT OF ESI

1. **Experimental details**
2. **Figure S1.** XRD patterns for (a) Z5, (b) 10A/Z5 and (c) 15A/Z5.
3. **Figure S2.** XPS spectra of the (a) Zn 2p, (b) In 3d and (c) S 2p in the Z1, 3A/Z1, Z5 and 3A/Z5 samples.
4. **Figure S3.** (a) XPS survey spectra, (b) Ag 3d, (c) Zn 2p, (d) In 3d and (e)S 2p of the Z5, 3A/Z5 and 10A/Z5 samples.
5. **Figure S4.** XPS spectra of Ag 3d of the Z1, 3A/Z1, Z5 and 3A/Z5 samples.
6. **Figure S5.** SEM images of ZIS.
7. **Figure S6.** (a) TEM image and (b) HRTEM image of the 100A/Z5.
8. **Figure S7.** (a) N_2 adsorption–desorption isotherms and (b) the pore size distribution curve of Z1, 3A/Z1, Z5, 3A/Z5.
9. **Figure S8.** Tauc plots of Z1 and Z5 (Figure S4).
10. **Figure S9.** XPS valence spectra of (a) Z1, (b) Z5 and (c) Ag_2S.
11. **Figure S10.** Energy band diagram of Z1, Z5 and Ag_2S.
12. **Figure S11.** H_2 evolution rates of (a) Z5, (b) 1A/Z5, (c) 3A/Z5 (d) 5A/Z5 and (e) 10A/Z5.
13. **Figure S12.** The optimized structures of (a) Z1 and (5) Z5.
14. **Figure S13.** Current–potential curves for photoelectrodes made of Z1, 3A/Z1, Z5 and 3A/Z5 measured in an aqueous solution without Na_2SO_3 (pH =6.8).
15. **Figure S14.** Theoretical photocurrent intensity of (a) Z1, (b) 3A/Z1, (c) Z5 and (d) 3A/Z5 according to light absorption.

16. **Figure S15.** Photoluminescence spectra of Z1, 3A/Z1 Z5 and 3A/Z5.

17. **Table S1.** Comparison of AQY of ZIS based- photocatalyst from recent publications.

18. **Table S2.** The average lifetimes of photogenerated charges of samples.

Experimental details

1. Characterization

Inductively coupled plasma optical emission spectrometry (ICP-OES, Thermo Scientific, iCAP 7400) was applied to detect the accurate molar ratios of Ag_2S. A Rigaku D/max-2000 diffractometer using Cu Kα1 radiation (λ = 0.15406 nm) was used to characterize the crystal structure of the as-prepared samples. To investigate the chemical composition and valence spectra of samples, X-ray photoelectron spectroscopy (XPS) analysis was conducted on a Thermo Scientific ESCALAB 250Xi X-ray photoelectron spectrometer with 20 eV pass energy with monochromatic Al Kα radiation (1486.6 eV). A HELIOS NanoLab 600i field emission scanning electron microscope (FE-SEM), a TALOS F200× field emission low-magnification transmission electron microscope (TEM), and high-resolution transmission electron microscopy (HRTEM) were applied to observe the morphologies of samples. The Brunauer-Emmett-Teller (BET) surface area and the Barrett-Joyner-Halenda (BJH) pore size distribution of the samples were acquired based on the nitrogen adsorption/desorption isotherms at 77 K (BET, Micromeritics ASAP2020, USA). The optical absorption of samples was recorded by an UV−vis spectrophotometer (HITACHI UH-4150) using $BaSO_4$ as a reference. Time-resolved fluorescence decay spectra were measured on a HORIBA FluoroMax-4 operating at room temperature.

2. Photocatalytic activity test

20 mg of a photocatalyst was dispersed in 50 mL of the aqueous solution which contained 0.35 M $Na_2S{\cdot}9H_2O$, and 0.25 M Na_2SO_3. The system was vacuumed before the photocatalytic reaction to remove all air. A 300 W Xe lamp (Trust-tech PLS-SXE 300, Beijing) equipped with a cut-off filter ($\lambda > 420$ nm) was used to provide the visible light irradiation. During the measurement, the temperature of the reactor was maintained at 279 K by providing cooling water. The amount of produced H_2 gas was determined using gas chromatography (Agilent 7890A) with a thermal conductivity detector (TCD).

The apparent quantum yield (AQY) for H_2 production was also measured under the same reaction conditions, only with light source passing through a 380, 420, 450, 475 and 500 nm band-pass filter. The irradiation area was controlled at 28 cm^2. The distance between the light source and the solution was 10 cm.

$$AQY(\%) = \frac{2 \times number\ of\ H_2\ molecules\ evoluved}{Number\ of\ incident\ photons} \times 100\%$$

The number of incident photons was calculated by a radiometer (Photoelectric Instrument Factory, Beijing Normal University).

3. Photoelectrochemical test

Current–potential curves and electrochemical impedance spectrum were measured with a three-electrode system using Pt and Ag/AgCl electrodes as the counter and reference electrodes, respectively. A spin-coating method was used to prepare working electrodes, and FTO glass (2 cm×2 cm) was used as a conducting substrate. A 300 W Xe lamp (Trust-tech PLS-SXE 300, Beijing) equipped with a cut-off filter ($\lambda > 420$ nm) was used as a light source and a 1 M Na_2SO_4 aqueous solution (100 mL, pH=5.91) or 1 M Na_2SO_4 with 1 M Na_2SO_3

(100 mL, pH=9.43) was used as the electrolyte solution. An AUTOLAB-PGSTAT302N electrochemical working station was used to manage the electrode's potential.

4. Theoretical methods

First-principles calculations based on density functional theory (DFT) were performed using the Vienna Ab initio Simulation Package (VASP). Electron-ion interactions were described by projector augmented wave (PAW) approach. Exchange-correlation interactions between electrons were treated by the generalized gradient approximation (GGA) with the Perdew-Burke-Ernzerhof (PBE) functional and the Heyd-Scuseria-Ernzerhof (HSE06) hybrid functional. The kinetic-energy cut-off of plane wave basis set was set 500 eV. Gamma-centered Monkhorst-Pack grids of 5 × 5 × 1 were used to sample the first Brillouin zone. The structures were optimized with total energy and force convergence standards of 10-4 eV and 10-2 eV/Å.

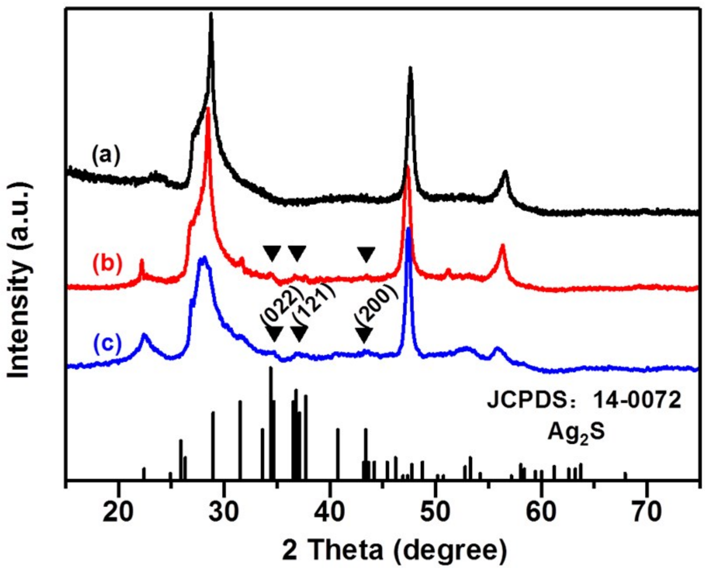

Figure S1. XRD patterns for (a) Z5, (b) 10A/Z5 and (c) 15A/Z5.

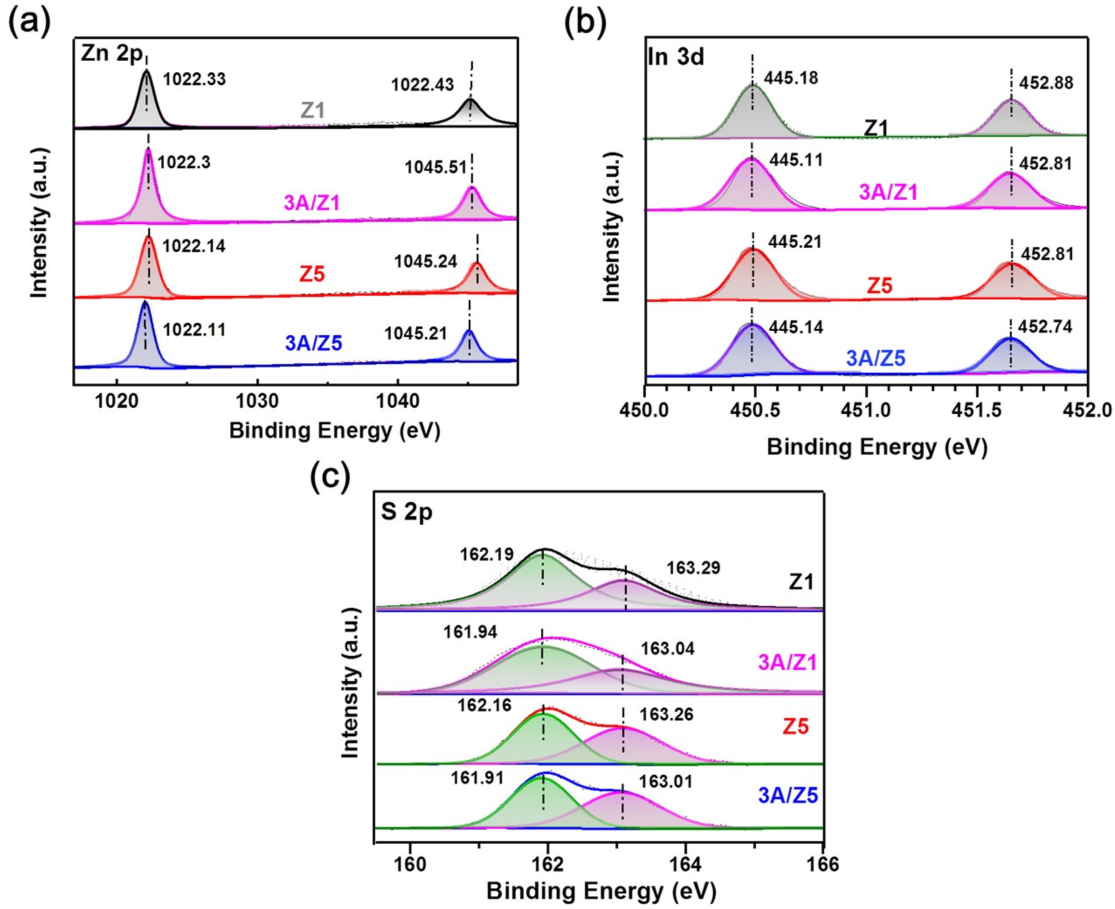

Figure S2. XPS spectra of the (a) Zn 2p, (b) In 3d and (c) S 2p in the Z1, 3A/Z1, Z5 and 3A/Z5 samples.

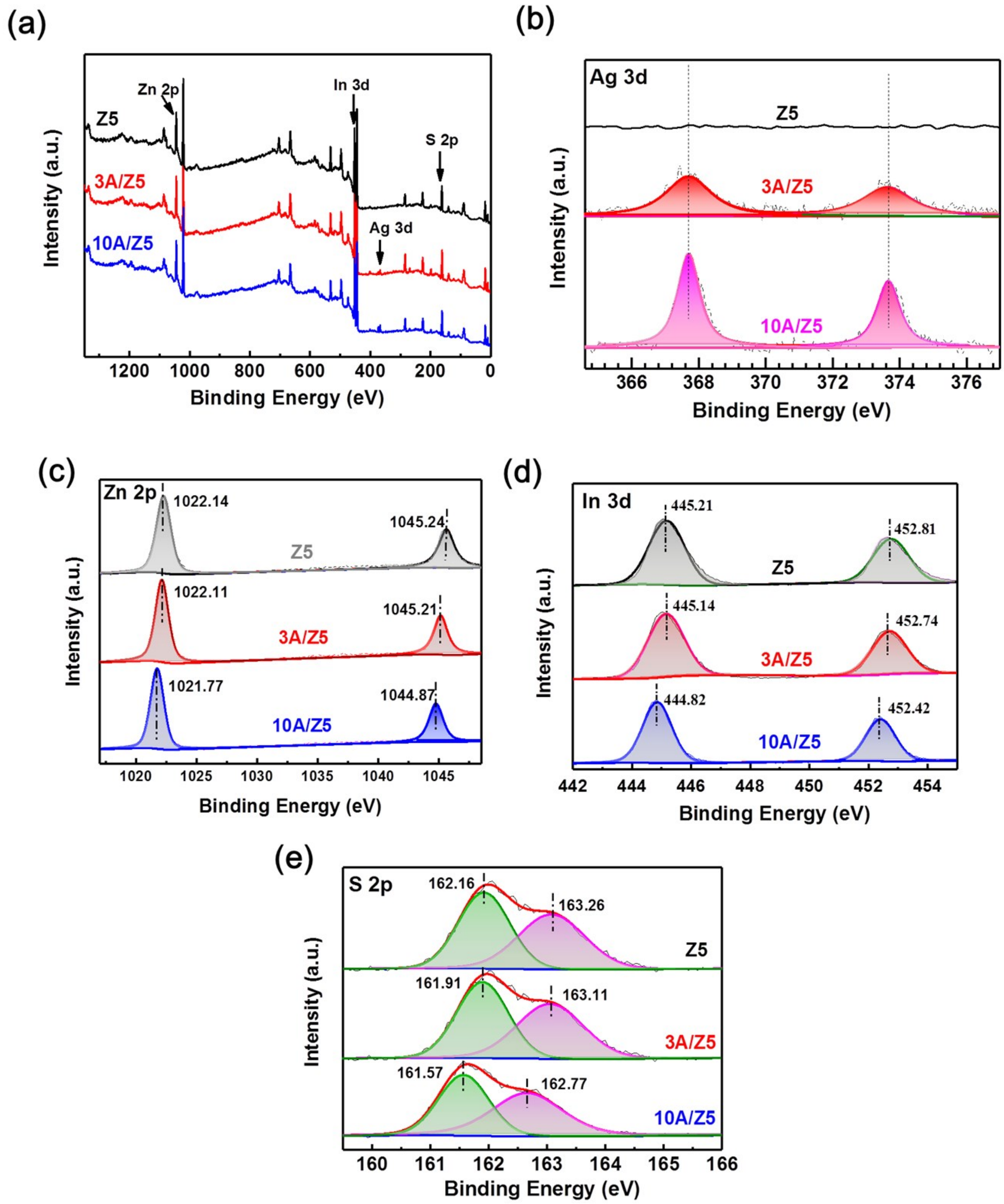

Figure S3. (a) XPS survey spectra, (b) Ag 3d, (c) Zn 2p, (d) In 3d and (e)S 2p of the Z5, 3A/Z5 and 10A/Z5 samples.

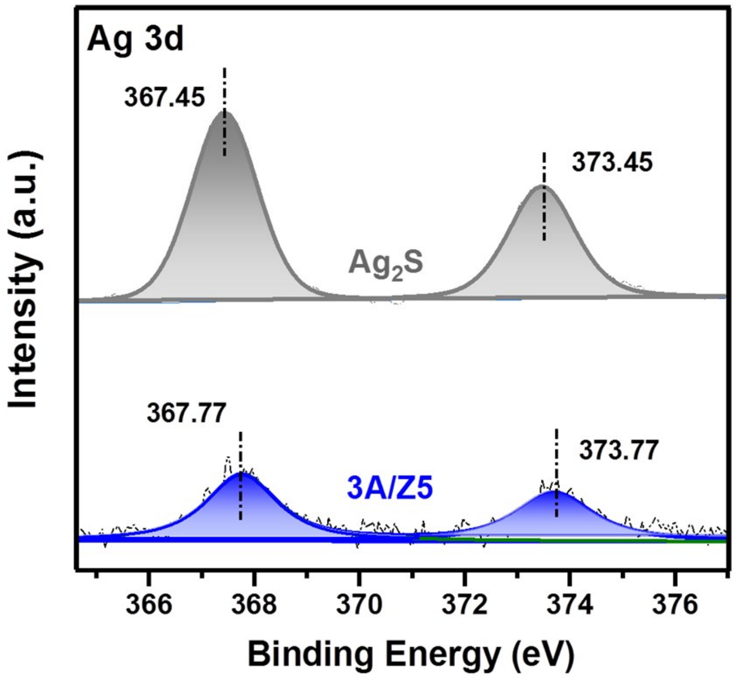

Figure S4. XPS spectra of Ag 3d of the Z1, 3A/Z1, Z5 and 3A/Z5 samples.

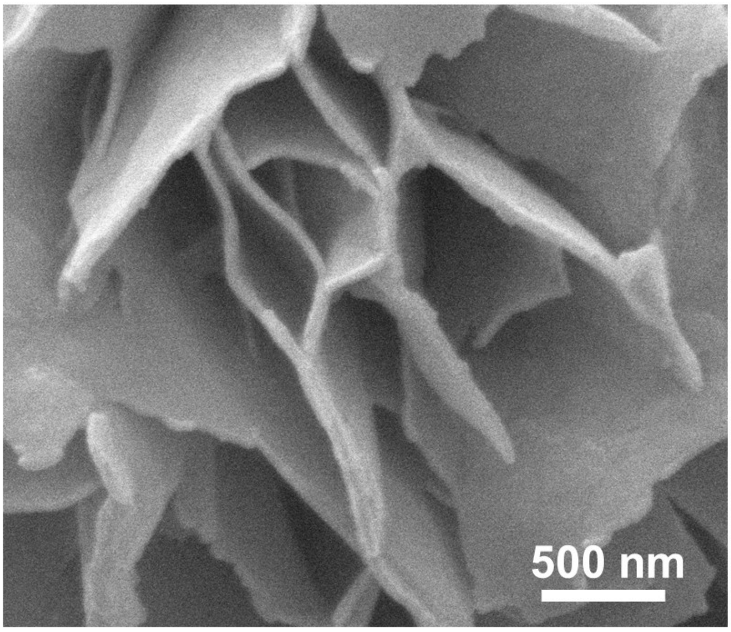

Figure S5. SEM images of ZIS.

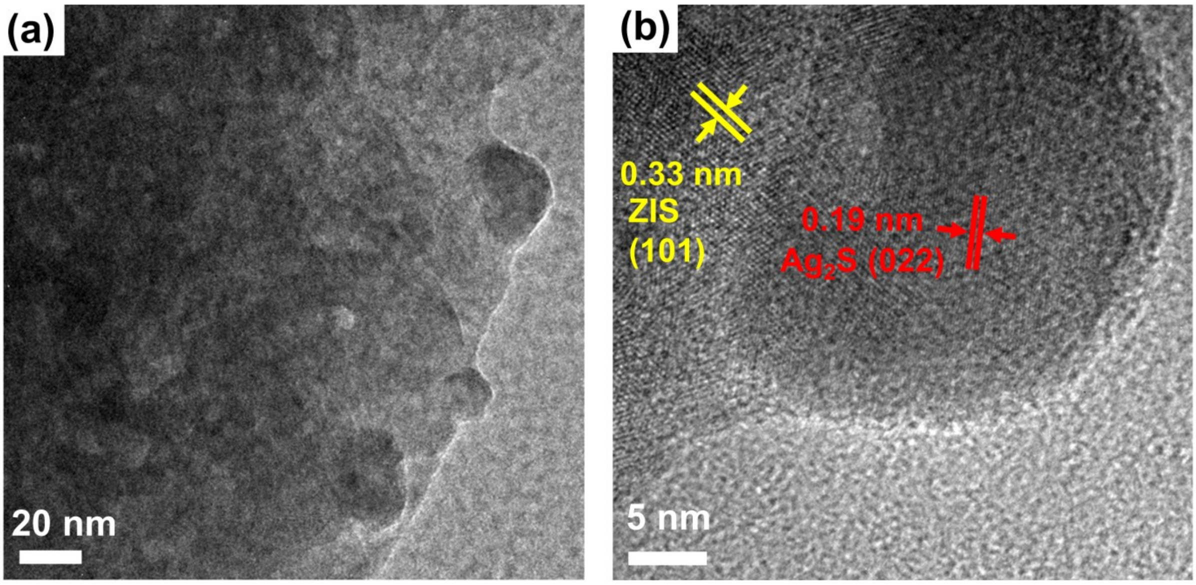

Figure S6. (a) TEM image and (b) HRTEM image of the 100A/Z5.

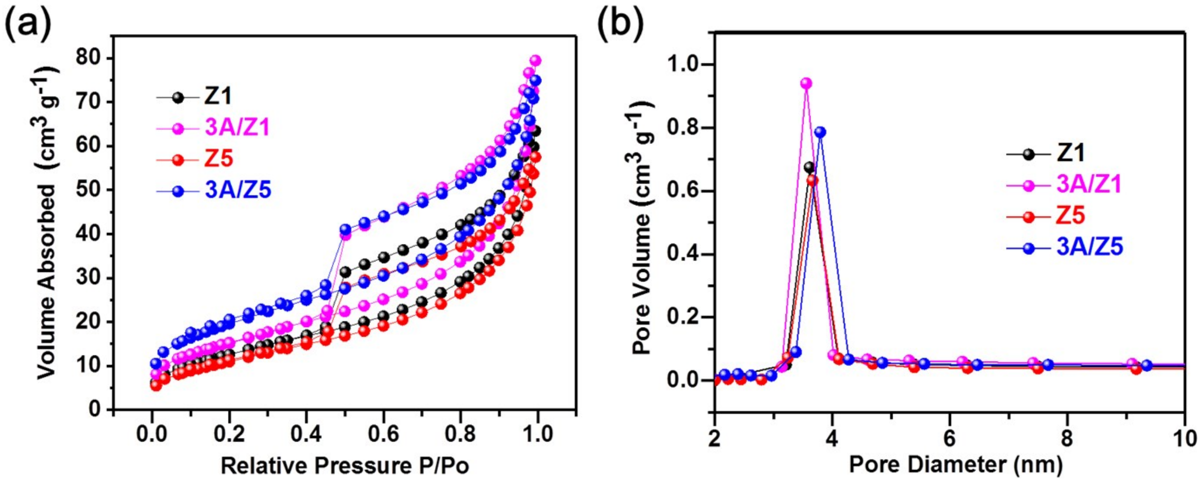

Figure S7. (a) N_2 adsorption–desorption isotherms and (b) the pore size distribution curve of Z1, 3A/Z1, Z5, 3A/Z5.

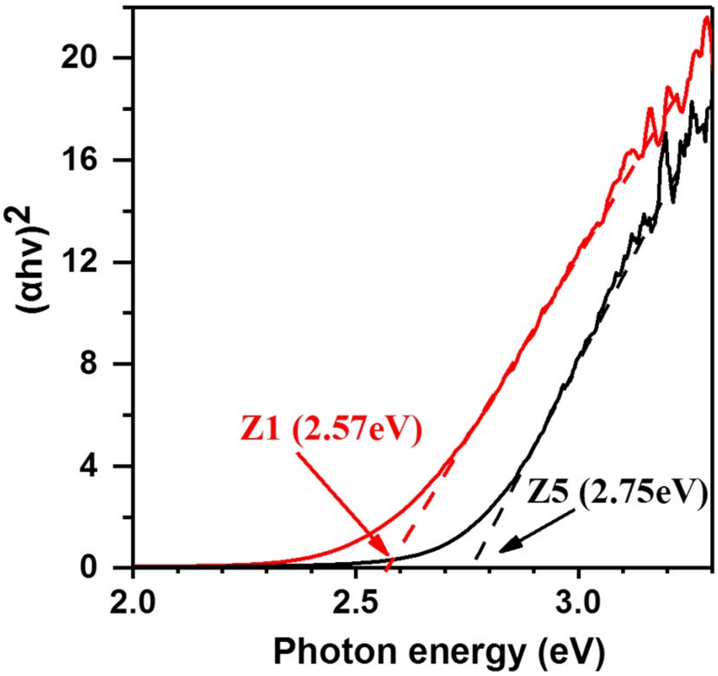

Figure S8. Tauc plots of Z1 and Z5.

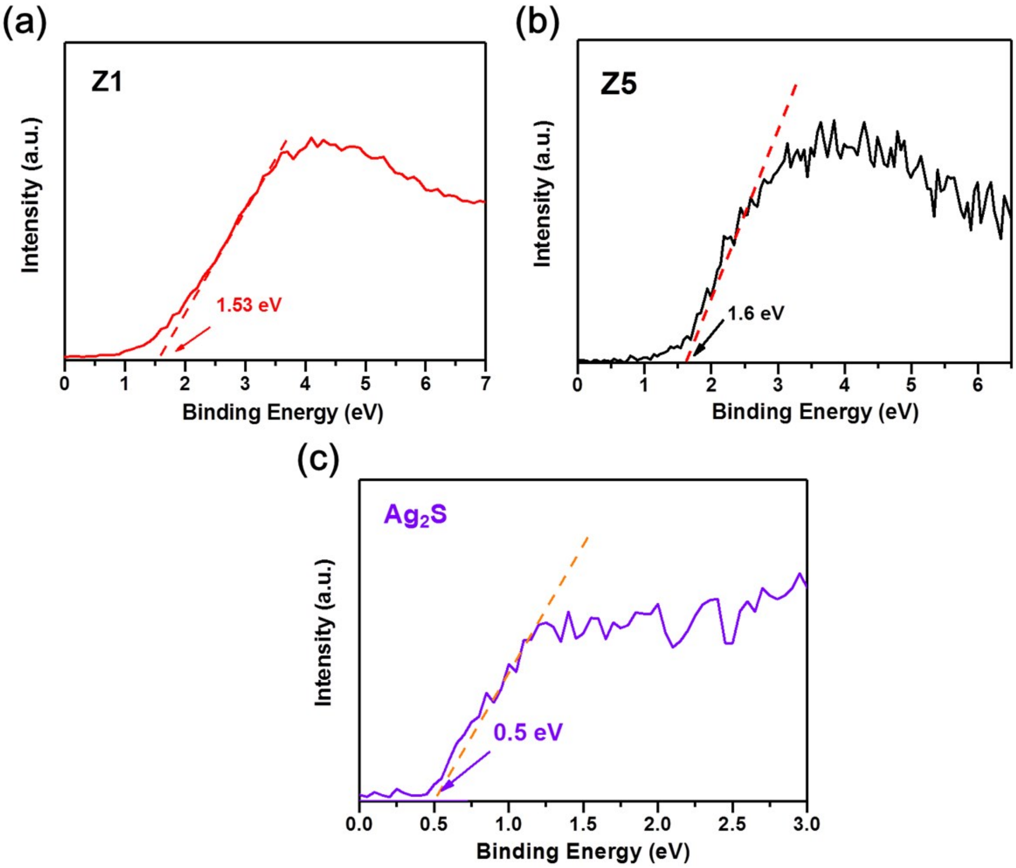

Figure S9. XPS valence spectra of (a) Z1, (b) Z5 and (c) Ag_2S.

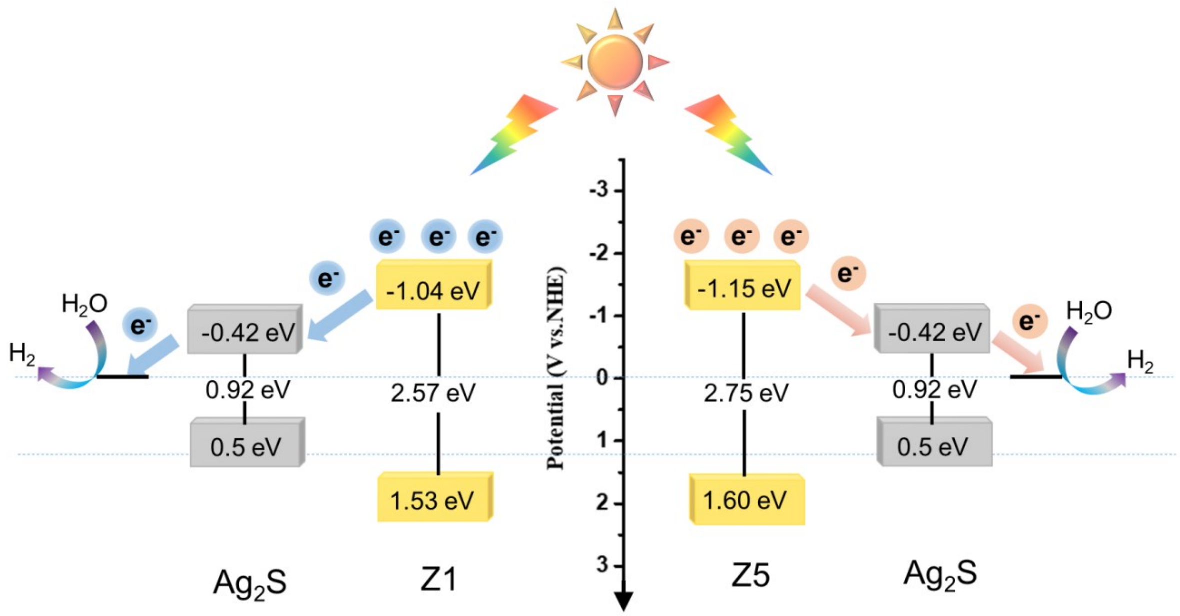

Figure S10. Energy band diagram of Z1, Z5 and Ag_2S.

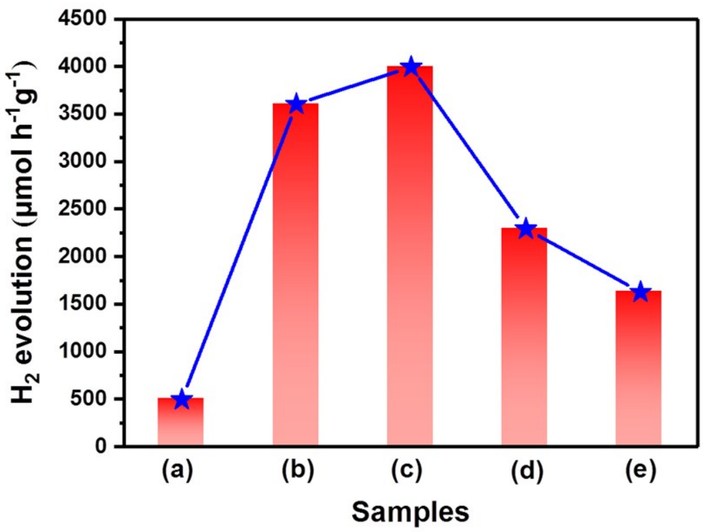

Figure S11. H_2 evolution rates of (a) Z5, (b) 1A/Z5, (c) 3A/Z5 (d) 5A/Z5 and (e) 10A/Z5.

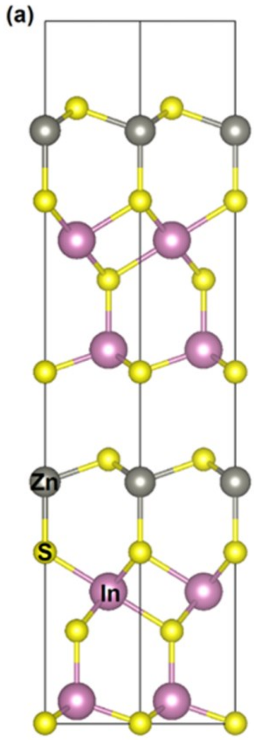

Figure S12. The optimized structures of (a) Z1 and (5) Z5.

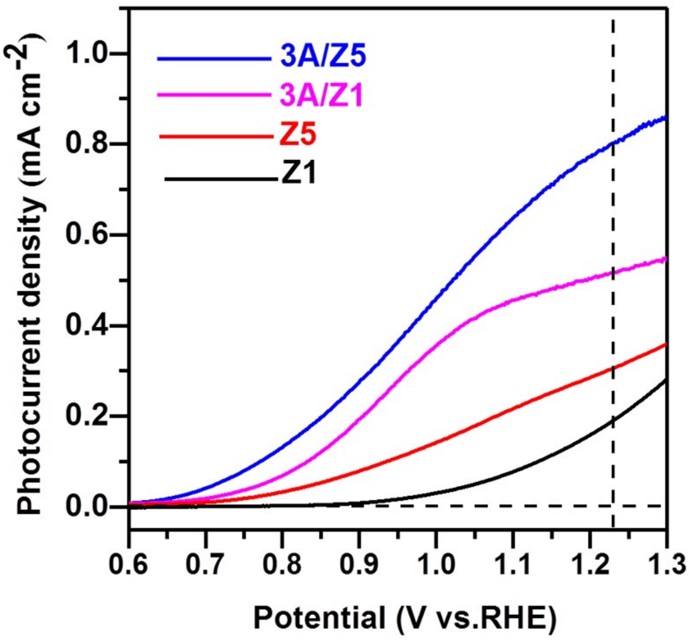

Figure S13. Current–potential curves for photoelectrodes made of Z1, 3A/Z1, Z5 and 3A/Z5 measured in an aqueous solution without Na_2SO_3 (pH =6.8).

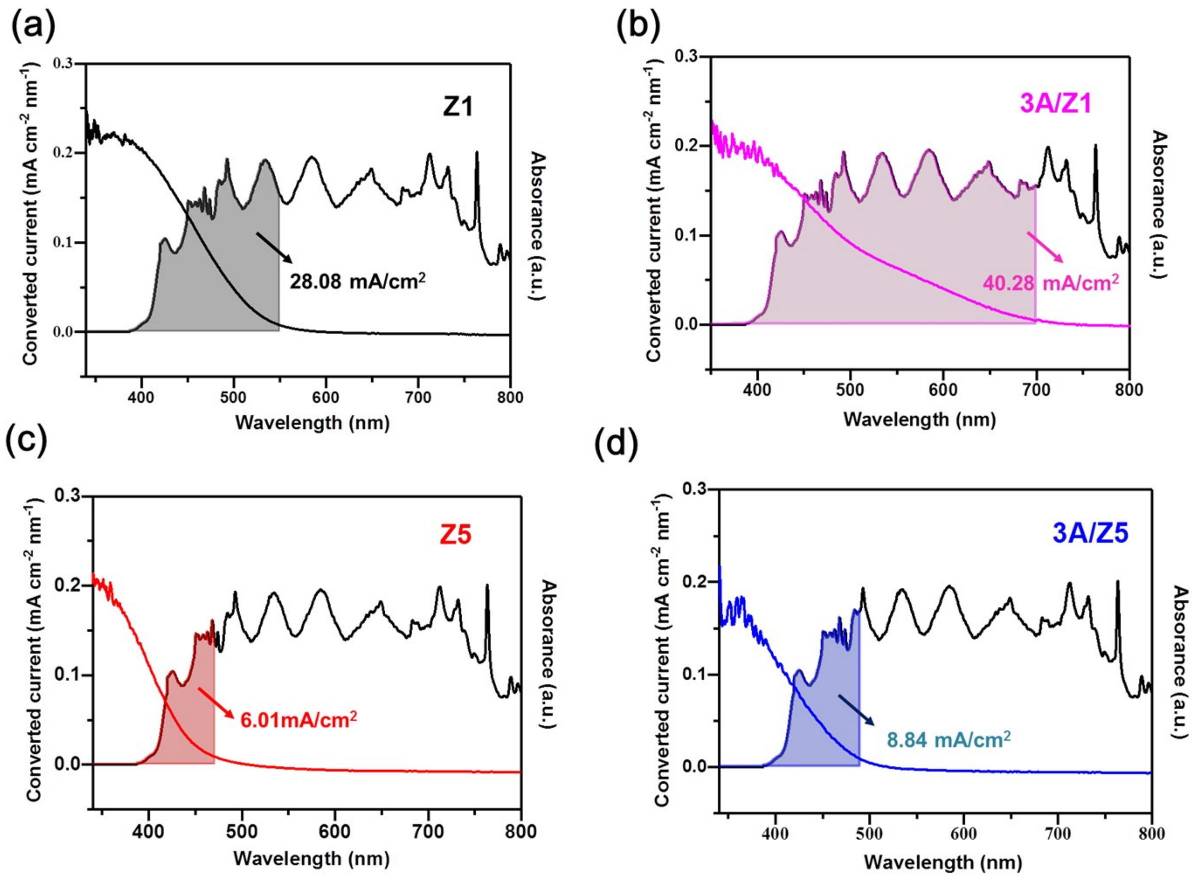

Figure S14. Theoretical photocurrent intensity of (a) Z1, (b) 3A/Z1, (c) Z5 and (d) 3A/Z5 according to light absorption.

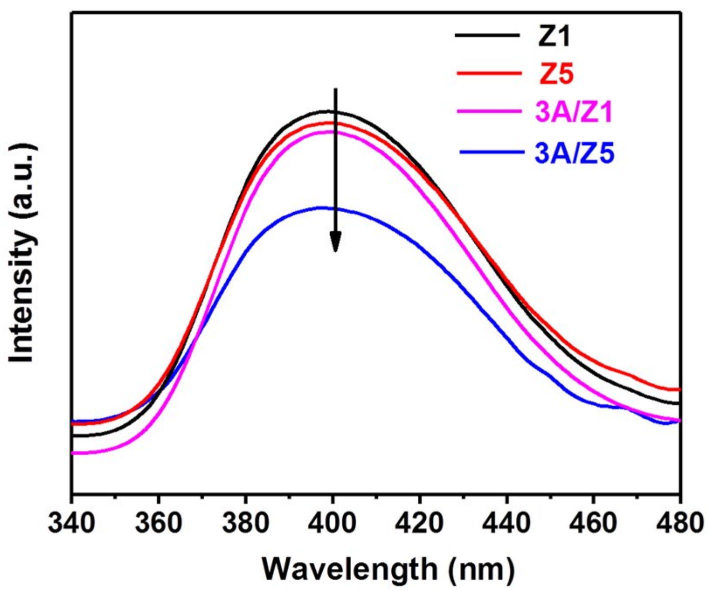

Figure S15. Photoluminescence spectra of Z1, 3A/Z1 Z5 and 3A/Z5.

Table S1. Comparison of AQY of ZIS based- photocatalyst from recent publications.

Ref	photocatalysts	Sacrificial agent	Wavelength (nm)	AQY (%)
This work	3A/Z5	Na_2S/Na_2SO_3	420	13.76
1	S-defect-controlled $ZnIn_2S_4$	TEOA	420	0.16
2	Pd@UiO-66-NH_2@$ZnIn_2S_4$	TEOA	420	3.2
3	$ZnIn_2S_4/BiVO_4$	TEOA	420	4.23
4	0.9%Ni/ $ZnIn_2S_4$-RVs	TEOA	420	9.6
5	$CdS/ZnIn_2S_4$	Na_2S/Na_2SO_3	420	15.9
6	Ni_x-ZIS	TEOA	420	17.10
7	MoS_2/CQDs/$ZnIn_2S_4$	TEOA	420	25.60

Table S2. The average lifetimes of photogenerated charges of samples.

Samples	τ_1 (ns)	τ_2 (ns)	A_1 (%)	A_2 (%)	Ave. τ (ns)
Z1	0.325	3.289	90.61	9.39	1.842
3A/Z1	0.304	4.863	90.57	9.43	3.153
Z5	0.452	4.911	95.87	4.13	1.875
3A/Z5	0.0947	9.450	95.40	4.60	7.840

REFERENCE

(1) J. Pan, G. Zhang, Z. Guan, Q. Zhao, G. Li, J. Yang, Q. Li, Z. Zou, *J. Energy Chem.* 2021, **58**, 408-414.

(2) M.T. Cao, F.L. Yang, Q. Zhang, J.H. Zhang, L. Zhang, L.F. Li, X.H. Wang, W.L. Dai, *J. Mater. Sci. Technol.* 2021, **76**, 189-199

(3) J.D. Hu, C. Chen, Z. Yang, G.P. Zhang, C.X. Guo, C.M. Li, *Small*, 2020,**16**, 2002988.

(4) X. Jing, N. Lu, J. Huang, P. Zhang, Z. Zhang, *J. Energy Chem.* 2021, **58**, 397-407.

(5) Y. Zhu, J. Chen, L. Shao, X. Xia, Y. Liu, L. Wang, *Appl. Catal. B: Environ.* 2020, **268**, 118744-118754.

(6) X. Shi, L. Mao, C. Dai, P. Yang, J. Zhang, F. Dong, L. Zheng, M. Fujitsuka, H. Zheng, *J. Mater. Chem. A* 2020, **8**, 13376-13384.

(7) B. Wang, Z. Deng, X. Fu, Z. Li, *J. Mater. Chem. A* 2018, **6**, 19735-19742.